

Search for light WIMP captured in the Sun using contained events in Super-Kamiokande

KOUN. CHOI¹⁹, K. ABE^{1,2}, Y. HAGA¹, Y. HAYATO^{1,2}, K. IYOGI¹, J. KAMEDA^{1,2}, Y. KISHIMOTO^{1,2}, M. MIURA^{1,2}, S. MORIYAMA^{1,2}, M. NAKAHATA^{1,2}, Y. NAKANO¹, S. NAKAYAMA^{1,2}, H. SEKIYA^{1,2}, M. SHIOZAWA^{1,2}, Y. SUZUKI^{1,2}, A. TAKEDA^{1,2}, T. TOMURA^{1,2}, R. A. WENDELL^{1,2}, T. IRVINE³, T. KAJITA^{2,3}, I. KAMETANI³, K. KANEYUKI, K. P. LEE³, Y. NISHIMURA³, K. OKUMURA^{2,3}, T. MCLACHLAN³, L. LABARGA⁴, E. KEARNS^{2,5}, J. L. RAAF⁵, J. L. STONE^{2,5}, L. R. SULAK⁵, S. BERKMAN⁶, H. A. TANAKA⁶, S. TOBAYAMA⁶, M. GOLDBABER, G. CARMINATI⁷, W. R. KROPP⁷, S. MINE⁷, A. RENSHAW⁷, M. B. SMY^{7,2}, H. W. SOBEL^{7,2}, K. S. GANEZER⁸, J. HILL⁸, N. HONG⁹, J. Y. KIM⁹, I. T. LIM⁹, T. AKIRI¹⁰, A. HIMMEL¹⁰, K. SCHOLBERG^{10,2}, C. W. WALTER^{10,2}, T. WONGJIRAD¹⁰, T. ISHIZUKA¹¹, S. TASAKA¹², J. S. JANG¹³, J. G. LEARNED¹⁴, S. MATSUNO¹⁴, S. N. SMITH¹⁴, T. HASEGAWA¹⁵, T. ISHIDA¹⁵, T. ISHII¹⁵, T. KOBAYASHI¹⁵, T. NAKADAIRA¹⁵, K. NAKAMURA^{15,2}, Y. OYAMA¹⁵, K. SAKASHITA¹⁵, T. SEKIGUCHI¹⁵, T. TSUKAMOTO¹⁵, A. T. SUZUKI¹⁶, Y. TAKEUCHI¹⁶, C. BRONNER¹⁷, S. HIROTA¹⁷, K. HUANG¹⁷, K. IEKI¹⁷, M. IKEDA¹⁷, H. KIKAWA¹⁷, A. MINAMINO¹⁷, T. NAKAYA^{17,2}, K. SUZUKI¹⁷, S. TAKAHASHI¹⁷, Y. FUKUDA¹⁸, Y. ITOW¹⁹, G. MITSUKA¹⁹, P. MIJAKOWSKI²⁰, J. HIGNIGHT²¹, J. IMBER²¹, C. K. JUNG²¹, C. YANAGISAWA²¹, H. ISHINO²², A. KIBAYASHI²², Y. KOSHIO²², T. MORI²², M. SAKUDA²², T. YANO²², Y. KUNO²³, R. TACIK²⁴, S. B. KIM²⁵, H. OKAZAWA²⁶, Y. CHOI²⁷, K. NISHIJIMA²⁸, M. KOSHIBA²⁹, Y. TOTSUKA²⁹, M. YOKOYAMA^{29,2}, K. MARTENS², LL. MARTI², M. R. VAGINS^{2,7}, J. F. MARTIN³⁰, P. DE PERIO³⁰, A. KONAKA³¹, M. J. WILKING³¹, S. CHEN³², Y. ZHANG³², R. J. WILKES³³ FOR THE SUPER-KAMIOKANDE COLLABORATION.

¹ Kamioka Observatory, Institute for Cosmic Ray Research, University of Tokyo, Kamioka, Gifu 506-1205, Japan ² Kavli Institute for the Physics and Mathematics of the Universe (WPI), Todai Institutes for Advanced Study, University of Tokyo, Kashiwa, Chiba 277-8582, Japan ³ Research Center for Cosmic Neutrinos, Institute for Cosmic Ray Research, University of Tokyo, Kashiwa, Chiba 277-8582, Japan ⁴ Department of Theoretical Physics, University Autonoma Madrid, 28049 Madrid, Spain ⁵ Department of Physics, Boston University, Boston, MA 02215, USA ⁶ Department of Physics and Astronomy, University of British Columbia, Vancouver, BC, V6T1Z4, Canada ⁷ Department of Physics and Astronomy, University of California, Irvine, Irvine, CA 92697-4575, USA ⁸ Department of Physics, California State University, Dominguez Hills, Carson, CA 90747, USA ⁹ Department of Physics, Chonnam National University, Kwangju 500-757, Korea ¹⁰ Department of Physics, Duke University, Durham NC 27708, USA ¹¹ Junior College, Fukuoka Institute of Technology, Fukuoka, Fukuoka 811-0295, Japan ¹² Department of Physics, Gifu University, Gifu, Gifu 501-1193, Japan ¹³ GIST College, Gwangju Institute of Science and Technology, Gwangju 500-712, Korea ¹⁴ Department of Physics and Astronomy, University of Hawaii, Honolulu, HI 96822, USA ¹⁵ High Energy Accelerator Research Organization (KEK), Tsukuba, Ibaraki 305-0801, Japan ¹⁶ Department of Physics, Kobe University, Kobe, Hyogo 657-8501, Japan ¹⁷ Department of Physics, Kyoto University, Kyoto, Kyoto 606-8502, Japan ¹⁸ Department of Physics, Miyagi University of Education, Sendai, Miyagi 980-0845, Japan ¹⁹ Solar Terrestrial Environment Laboratory, Nagoya University, Nagoya, Aichi 464-8602, Japan ²⁰ National Centre For Nuclear Research, 00-681 Warsaw, Poland ²¹ Department of Physics and Astronomy, State University of New York at Stony Brook, NY 11794-3800, USA ²² Department of Physics, Okayama University, Okayama, Okayama 700-8530, Japan ²³ Department of Physics, Osaka University, Toyonaka, Osaka 560-0043, Japan ²⁴ Department of Physics, University of Regina, 3737 Wascana Parkway, Regina, SK, S4S0A2, Canada ²⁵ Department of Physics, Seoul National University, Seoul 151-742, Korea ²⁶ Department of Informatics in Social Welfare, Shizuoka University of Welfare, Yaizu, Shizuoka, 425-8611, Japan ²⁷ Department of Physics, Sungkyunkwan University, Suwon 440-746, Korea ²⁸ Department of Physics, Tokai University, Hiratsuka, Kanagawa 259-1292, Japan ²⁹ The University of Tokyo, Bunkyo, Tokyo 113-0033, Japan ³⁰ Department of Physics, University of Toronto, 60 St., Toronto, Ontario, M5S1A7, Canada ³¹ TRIUMF, 4004 Wesbrook Mall, Vancouver, BC, V6T2A3, Canada ³² Department of Engineering Physics, Tsinghua University, Beijing, 100084, China ³³ Department of Physics, University of Washington, Seattle, WA 98195-1560, USA

suzuki@icrr.u-tokyo.ac.jp

Abstract: Super-Kamiokande can search for dark matter by detecting neutrinos and muons which are produced by WIMP pair annihilations occur inside the Sun. The huge gravity and hydrogen-rich composition of the Sun combined with high sensitivity of Super-Kamiokande for low energy (few GeV) neutrinos allow us good sensitivity to light (few GeV to few 10 GeV) WIMP dark matter, especially for spin-dependent coupling case. In this analysis, we increased signal acceptance by using fully-contained and partially-contained neutrino events added to up-going muons in Super-Kamiokande. We also used minimum χ^2 method to use energy, direction and flavor informations. We fitted Super-Kamiokande I-IV data to find the allowed contribution of WIMP-induced neutrino events added to large back-ground of atmospheric neutrino events. As a result, we found no signal observed and the null result was interpreted as upper limit on the spin-dependent (SD) WIMP-proton elastic scattering cross-section for $\chi\chi \rightarrow b\bar{b}$ and $\chi\chi \rightarrow \tau^+\tau^-$ WIMP annihilation channels. We set current best limit for WIMP mass below 100 GeV.

Keywords: Super-Kamiokande, indirect WIMP search.

1 Introduction

As a candidate for non-baryonic cold dark matter particle arising from rich cosmological motivations, weakly interacting massive particles (WIMPs) are naturally favored as their thermal relic abundance is automatically of the right order of magnitude (WIMP miracle). Moreover, it is motivated in supersymmetric or dimensional extensions of the Standard Model of particle physics. A promising way to identify the WIMP-like dark matter particle is to search for excess neutrino flux from the Sun generated by self-annihilation of WIMPs inside the Sun. As the Sun travels on the Milky Way arm, WIMPs may get gravitationally bound if they lose energy by scattering off nuclei in the Sun, and pair-annihilate in deep core in which produced neutrinos can propagate and be detected in terrestrial detectors. Considering interactions inside the Sun and the Earth, oscillation effects during propagation, the WIMP Monte Carlo simulator DarkSUSY [1] and WimpSim [2] calculate WIMP-induced neutrino flux in neutrino detector. Thanks to hydrogen-rich composition and huge gravity of the Sun, tight limits on spin-dependent scattering (SD) cross-section have been placed with neutrino telescopes.

Neutrino detectors usually interpret their null results of excess neutrino observation as upper limits on WIMP-nucleon scattering cross-section assuming pair annihilation to mono annihilation channel of fermions, axial vector (SD) or scalar coupling (SI) only elastic scattering type which conserves isospin, equilibrium achieved between capture rate and annihilation rate. These assumptions help to interpret our result in model-independent way and to compare it with other detector results. We also assume a standard dark matter halo of local density $0.3 \text{ GeV}/\text{cm}^3$, Maxwellian velocity distribution of WIMPs with RMS velocity of 270 km/s and circular velocity of solar system of 220 km/s .

Accumulating signal claims from direct detections DAMA, CoGeNT, CRESST, CDMS-Si for 5~20 GeV WIMP and conflicting null results from CDMS-Ge, XENON10/100, IceCube, Simple, PICCASO, etc became a motivation for study of light WIMP. As recent theoretical works [3, 4] indicate, taking advantage of sensitivity for few GeV neutrino, Super-Kamiokande (SK) is expected to have strong power to examine WIMPs with mass of few GeV to few 10 GeV. To exploit sensitivity to few GeV neutrino, our analysis is updated to use contained neutrino events, and the first result using SK I-IV data will be presented. Focusing on light WIMP search, we scanned WIMP mass from 4 GeV to 200 GeV. Among fermion annihilation channels expected to yield competitive neutrino flux, $\tau^+\tau^-/b\bar{b}$ channels are selected to represent most strong/conservative cases. For $b\bar{b}$ channel, candidates start from 6 GeV due to kinematic constraint.

The outline of this paper is as follows. A review of the SK detector is presented in Sec. 2. Analysis strategy is explained in Sec. 3, method in detail is described in Sec. 4. The result of the analysis on neutrino flux upper limit will be shown and interpreted as WIMP-nucleon scattering cross-section in Sec. 5. Finally, Sec. 6 concludes.

2 Super-Kamiokande detector and event details

Super-Kamiokande is a cylindrical water Cherenkov detector located in the Kamioka mine in Japan. The inner detec-

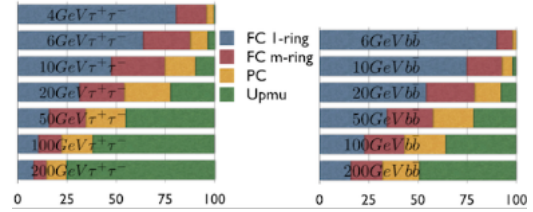


Figure 1: Signal fraction in SK event categories for candidate WIMPs, for $\tau^+\tau^-$ channel (left) & $b\bar{b}$ channel (right).

tor (ID) of 22.5ktons fiducial volume is covered with approximately 11,100 (5200 for SK-II) 21-inch Hamamatsu photomultiplier tubes (PMTs) and the outer detector (OD) covered with 1,885 8-inch PMTs is used as a veto. Information on experimental setup of the detector and calibration are provided in [5].

The Super-Kamiokande high-energy neutrino (visible energy (E_{vis}) $> 30 \text{ MeV}$) data are divided into three categories: Fully contained (FC) events which deposit all of their Cherenkov light in the ID, partially contained (PC) events which additionally have an exiting particle that deposits energy in the OD, upward-going muon (up- μ)s which are produced by neutrino interactions in the surrounding rocks of the detector, in which muons either stop in the detector (stopping up- μ), or pass through the detector (through-going up- μ). Through-going up- μ events are subdivided into showering and nonshowering. FC and PC events are also further divided into sub-categories. Detailed information on event categorization, reconstruction and reduction can be found in SK atmospheric neutrino oscillation analysis description [5].

This analysis uses data accumulated during SK I-IV run periods. SK-I (1996 to 2001) FC/PC correspond to 1489 live-days and up- μ events correspond to 1646 days of live time. SK-II (2002 to 2005) had 799 live-days of FC/PC and 828 live-days of up- μ events. SK-III (2005 to 2007) contains 518 live-days of FC/PC with 636 live-days of up- μ events. SK-IV (2007 to current) data taking is ongoing; in this analysis we used the data collected until March 2012, containing 1096.7 live-days of FC/PC/up- μ events. The details of each run periods will be found in [5]. Since the physical configuration of the detector and its reconstruction performance varies, separate 500 year Monte Carlo simulation (MC)s of atmospheric neutrino are generated for each SK run period. The primary atmospheric neutrino flux is taken from the Honda flux11 model [6] and neutrino interactions in the detector are generated using the NEUT simulator [7, 8] and GEANT-based detector simulator. More detailed explanation of the atmospheric neutrino MC is presented in [9, 10].

3 Analysis strategy

Previous Super-Kamiokande WIMP search [12] has been done using up- μ events which dominate SK data above 10 GeV, gaining good sensitivity for search for WIMPs in several tens of GeV to few TeV mass range. In case of lighter WIMPs, most of the signal will go to contained neutrino event (FC+PC) categories. Fig. 1 shows the expected signal fraction in SK event categories for candidate WIMP masses and channels used.

To increase signal acceptance, our analysis is updated

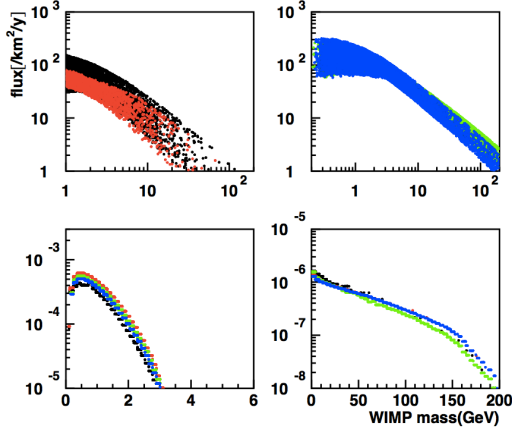


Figure 2: Top left : True energy spectrum of original atmospheric electron-neutrino flux (black) / anti-electron-neutrino flux (red). Top right : True energy spectrum of original atmospheric muon-neutrino flux (green) / anti-muon-neutrino flux (blue). Bottom left : True energy spectrum of mimicked WIMP-induced neutrino for 200 GeV $\tau^+\tau^-$ candidate (colors are same as above). Bottom right : True energy spectrum of mimicked WIMP-induced neutrino for 6 GeV $b\bar{b}$ candidate (colors are same as above).

to use FC and PC events as well, so all high-energy events collected in SK. Compared to previous analysis [12] the signal acceptance is increased 50 times for 10 GeV $b\bar{b}$ channel WIMP candidate. To reduce the overwhelming atmospheric neutrino back-ground (BG) events which increase as $\propto E^{-2.7}$, angular cut approach used in previous analysis is not as efficient because the resolution of neutrino direction is larger for contained and low-energy events. In this analysis, we adopt fitting approach whose format has been developed for SK atmospheric neutrino oscillation analysis. The different energy spectrum of the atmospheric neutrino back-ground and the signal, distinctive angular distribution of the signal peaking toward the direction of the Sun, and flavor ratio informations are fully used in the fitting approach to reduce back-ground. The details of the analysis will be described in next section.

4 Analysis method

Under the hypothesis that collected data consist of atmospheric neutrinos as well as of WIMP-induced neutrinos, we compare data to MC; MC originally generated for atmospheric neutrino is used in two ways - to predict atmospheric neutrino back-ground, and to mimic the WIMP-induced neutrino signal. For later, selected sample of MC events is weighted by the ratio of simulated WIMP-induced neutrino flux and the original atmospheric neutrino flux, in which way the flux information is replaced as leaving simulated detector response. WIMP-induced neutrino flux has fixed flavor ratio, energy spectrum calculated by DarkSUSY [1] and point-like direction coming from the Sun. Fig. 2 shows original atmospheric flux and mimicked WIMP-induced neutrino flux for representative WIMP candidates.

Back-ground are normalized by livetime of SK data. We consider three flavor oscillation for back-ground with $\sin^2 \theta_{13} = 0.025$, $\sin^2 \theta_{12} = 0.304$, $\sin^2 \theta_{23} = 0.425$, $\Delta m_{12}^2 = 7.66 \times 10^{-5}$, $\Delta m_{32}^2 = 2.66 \times 10^{-3}$. Tau MC [11] is

also used for atmospheric tau-neutrino back-ground generated in neutrino oscillation and for WIMP-induced tau-neutrino signal. The data and MC are further divided into 18 sub-samples which help to exploit different characteristics of signal from back-ground. Events in each sample are distributed in reconstructed momentum and angular bins. The sampling and binning basically follow atmospheric oscillation analysis [5], but for our purpose we define angle as the direction between reconstructed event direction and the direction from the Sun ($\cos\theta_{Sun}$) instead of zenith angle.

For each mass and annihilation channel of WIMP hypothesis, we compare data and MC using the least χ^2 -square method to find the allowed contribution of signal added to back-ground which best matches the data. One global parameter β without prior limit varies the overall normalization of the signal in pulled χ^2 method based on a Poisson probability distribution :

$$\chi^2 = 2 \sum_{n=1}^{\#ofbins} [N_n^{BG} (1 + \sum_j f_j^n \epsilon_j) + \beta N_n^\chi (1 + \sum_k f_k^n \epsilon_k) - N_n^{data} + N_n^{data} \ln \left(\frac{N_n^{data}}{N_n^{BG} (1 + \sum_j f_j^n \epsilon_j) + \beta N_n^\chi (1 + \sum_k f_k^n \epsilon_k)} \right)] + \sum_j \left(\frac{\epsilon_j}{\sigma_j} \right)^2 + \sum_k \left(\frac{\epsilon_k}{\sigma_k} \right)^2$$

where n is the index of the bins; N_n^{data} is the number of events observed in each bin; N_n^{BG} is the back-ground expectation in the bin; N_n^χ is the number of events of signal sample in the bin where β stands for the allowed fraction of it so that $\beta \times N_n^\chi$ is interpreted as allowed contribution of WIMP-induced neutrino in the bin.

The systematic errors are separately considered for back-ground and signal. j/k is the systematic uncertainty index for back-ground/signal ; σ_j/σ_k is the j -th/ k -th systematic error and ϵ_j/ϵ_k is the pull to them. f_j^n/f_k^n is the fractional change in the predicted back-ground/signal in the n -th bin due to 1σ change of the j -th/ k -th systematic error. For back-ground, most systematic uncertainties are shared with oscillation analysis, f_j^n values are borrowed from atmospheric oscillation analysis and rearranged in $\cos\theta_{Sun}$ bins. The list and detail of the systematic errors are explained in [5]; note that some errors relevant for zenith angle distribution are not used in this analysis. We also add 6 new errors for 5 oscillation parameters and matter effect inside the Earth. For the signal, σ_k s related to neutrino interaction, detector performance and event reconstruction/reduction are adopted from oscillation analysis. We added uncertainty in direction reconstruction studied using axial mass in neutrino interaction, considering susceptibility of directional information to search for point-like signal source. Uncertainties in oscillation/interaction/matter effect inside the Sun are considered by simulating the neutrino flux using WIMPSim as varying 10% of each oscillation parameter/interaction cross-section/electron density, and the f_k^n values are calculated based on difference compared to the nominal spectrum.

For each β , $N_n^{BG} + \beta N_n^\chi$ is recalculated to account for systematic uncertainties, as ϵ_j/ϵ_k are varied to minimize χ^2 . By calculating contribution of each bin to total χ^2 value and contribution from penalty term $\sum_j \left(\frac{\epsilon_j}{\sigma_j} \right)^2 + \sum_k \left(\frac{\epsilon_k}{\sigma_k} \right)^2$, we find best fit β_{min} for minimum $\Delta\chi^2$ value, and N_{90} , which is 90% upper limit of number of WIMP events allowed. When β_{min} lies in unphysical region, we follow Bayesian approach assuming flat priors which calculates 90% upper limit in positive region of β .

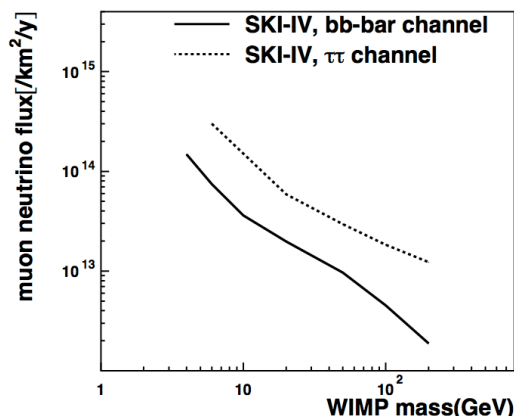


Figure 3: 90% Upper limit of WIMP-induced muon-neutrino flux. red : data (SK I-IV), black : sensitivity using toy MC.

5 Analysis result

We set 90% upper limit on WIMP-induced muon-neutrino flux. Fig. 3 shows the derived upper limit on WIMP-induced muon-neutrino flux.

Under the assumption of equilibrium between WIMP capture and annihilation in the Sun, amount of WIMP-induced neutrino flux scales with WIMP-nucleon scattering cross-section. Upper limit on SD WIMP-nucleon cross-section is derived using DarkSUSY [1]. We consider several source of uncertainties in capture process as listed in table 1. Uncertainty from form factor is relevant for scattering off heavy nuclei, which is expected to be negligible in SD scattering where only hydrogen plays important role. Solar diffusion effect is calculated using DarkSUSY [1] and found to be negligible for WIMPs in the mass range of our interest. To calculate uncertainty of solar composition, bs05op and bs05agsop models are compared using DarkSUSY. Solar evaporation has no impact above 4 GeV, and below 4 GeV is not used in the analysis. In conclusion, combining effects of all errors loosen the upper limit maximally 7% for high-mass WIMP. The upper limit on SD WIMP-proton cross-section is shown in Fig. 4 together with other experimental limits.

m_χ (GeV)	form factor	solar model	solar evaporation	solar diffusion
4~	1%	3%	1%	0%
50~	1%	4%	1%	0%
200	1%	6%	1%	3%

Table 1: Relative magnitudes of 1σ systematic uncertainties in SD scattering capture process of WIMPs in the Sun for different mass samples.

6 Conclusion

The first WIMP search using contained events in SK is shown. The result of the study is consistent with no signal from 10 GeV WIMP with SD coupling size of $1.1 \times 10^{-39} \text{ cm}^2 / 1.1 \times 10^{-40} \text{ cm}^2$ to proton when $\tau^+ \tau^- / b\bar{b}$ annihilation channels are assumed. The derived upper limit on

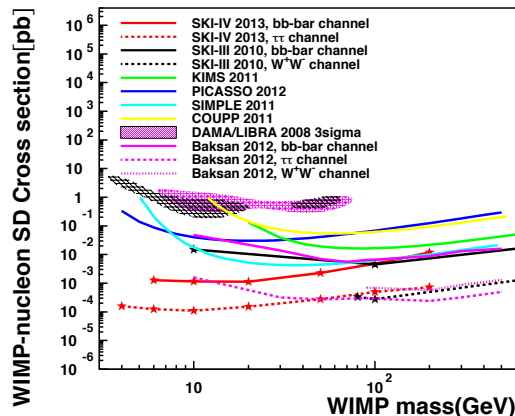


Figure 4: 90% Upper limit on SD WIMP-proton cross-section with limits from other detectors.

SD WIMP-proton cross-section shows the most stringent constraint to date for WIMP mass below 100 GeV.

References

- [1] Gondolo, P. and Edsjo, J. and Ullio, P. and Bergstrom, L. and Schelke, M. and Baltz, E.A., JCAP 07 (2004) 008
- [2] Edsjo, J., <http://www.fysik.su.se/~edsjo/wimpsim/>
- [3] Kappl, R. and Winkler, M. W., Nucl.Phys. B850 (2011) 505
- [4] Carsten, R. and Tanaka, T. and Itow, Y., JCAP 09 (2011) 029
- [5] Lee, K. P., <http://www-sk.icrr.u-tokyo.ac.jp/sk/pub/Lee>
- [6] Honda, M and Kajita, T. and Kasahara, K. and Midorikawa, S, Phys. Rev. D83 (2011) 123001
- [7] Hayato, Y., Nucl. Phys. Proc. Suppl. 112 (2002) 171 ; G. Mitsuka, AIP Conf. Proc. 967 (2007) 208; G. Mitsuka, AIP Conf. Proc. 981 (2008) 262
- [8] Mine, S. et al. (K2K), Phys. Rev. D77 (2008) 032003
- [9] Nishino, H. et al. (Super-Kamiokande), Phys. Rev. D85 (2011) 112001
- [10] Ashie, Y. et al. (Super-Kamiokande), Phys. Rev. D71 (2005) 112005
- [11] Abe, K. et al. (Super-Kamiokande), Phys. Rev. Lett. 110 (2012) 181802
- [12] Tanaka, T. et al. (Super-Kamiokande), Astrophys. J. 742 (2011) 78